11th International Conference on Fracture Mechanics of Concrete and Concrete Structures
FraMCoS-11
J. M. Chandra Kishen, A. Ramaswamy, S. Ray and R. Vidyasagar (Eds)
https://doi.org/10.21012/FC11.092369

COMPUTATIONAL MODELING OF DYNAMIC FRACTURE OF LAYERED COMPOSITE UNDER VARIOUS STRAIN-RATE LOADING

SOBHAN PATTAJOSHI*, SONALISA RAY†

*†Indian Institute of Technology
Roorkee, India
e-mail: sobhan_p@ce.iitr.ac.in

†Indian Institute of Technology
Roorkee, India
e-mail: sonalisa.ray@ce.iitr.ac.in

Key words: Layered composite, Dynamic fracture, Strain-rate variation, Protective bunker

Abstract. Generally layered composite target consisting of camouflage, fiber reinforced concrete (FRC), boulder-mixed cement mortar, ultra-high performance fiber reinforced concrete (UHPFRC), high-density polyethylene (HDPE), and reinforced concrete is employed as a protective bunker to safeguard military personnel from projectile impact loading. This research focuses on numerical modelling to analyze the dynamic fracture behavior and assess the structural integrity of the layered composite target under projectile impact. The results demonstrate that the layered composite target exhibits superior protection against projectile impact loading compared to a monolayer reinforced concrete target of equivalent thickness. Furthermore, the utilization of locally available boulders in the cement mortar layer enhances the penetration resistance of the layered composite target. Consequently, the layered composite target can be a suitable replacement for monolayer reinforced concrete targets of equivalent thickness in scenarios involving projectile impact loading.

1 INTRODUCTION

The computational modeling of dynamic fracture behavior in layered composite structures subjected to various strain-rate loadings is an area of significant research interest [1, 2]. Layered composites have gained attention due to their potential to provide enhanced resistance against projectile impact loading, making them suitable for military bunker applications. Understanding the fracture behavior of these structures under different loading conditions is crucial for optimizing their design and improving protective capabilities.

In military bunkers, the use of layered composites, which consist of multiple material layers, offers advantages over monolithic structures such as reinforced concrete (RC) or fiber-reinforced concrete (FRC) [3–8]. These composites typically comprise layers such as Camouflage, fiber reinforced concrete (FRC), boulder-mixed cement mortar, ultra-high performance fiber reinforced concrete (UHPFRC), high-density polyethylene (HDPE), and reinforced concrete. Each layer contributes specific properties to the overall structural response, providing a combination of strength, energy absorption, and penetration resistance.

This research aims to investigate the dynamic fracture behavior of layered composite structures and analyze their performance under various strain-rate loadings, particularly in the context of projectile impact. Computational modeling using advanced software tools, such as Ansys Autodyn, allows for detailed analysis of the damage mechanisms and structural response of the layered composite targets.

The objective of this study is to quantitatively assess the mechanical performance of the layered composite targets through numerical simulations. Parameters of interest include the velocity profiles of the impacting projectiles, residual velocities, penetration depths, crater diameters, and damage evaluation [9]. By comparing the results with those obtained from monolayer reinforced concrete targets of equivalent thickness, the effectiveness of the layered composites in providing enhanced protection can be evaluated.

Furthermore, this research investigates the fracture patterns within the layered composite structures, taking into account the variation in the strain-rate and material properties of each layer [10]. The behavior of the layered composites under different strain-rate loadings enables a deeper understanding of their response to dynamic fracture and aids in optimizing their design for improved performance.

The findings of this study will contribute to the advancement of computational modeling techniques for layered composite structures and provide valuable insights into their dynamic fracture behavior under various strain-rate loadings. By enhancing our understanding of these materials response to projectile impact, this research can inform the development of more robust and effective protective structures for military applications, particularly in scenarios where rapid loading and fracture are critical concerns.

2 MATERIALS AND METHODS

A numerical investigation was conducted to analyze the impact response of two types of targets subjected to impact velocity of 300 m/s of an ogival-nose steel projectile with a diameter of 50.80 mm [11] a shown in Fig.1(c).

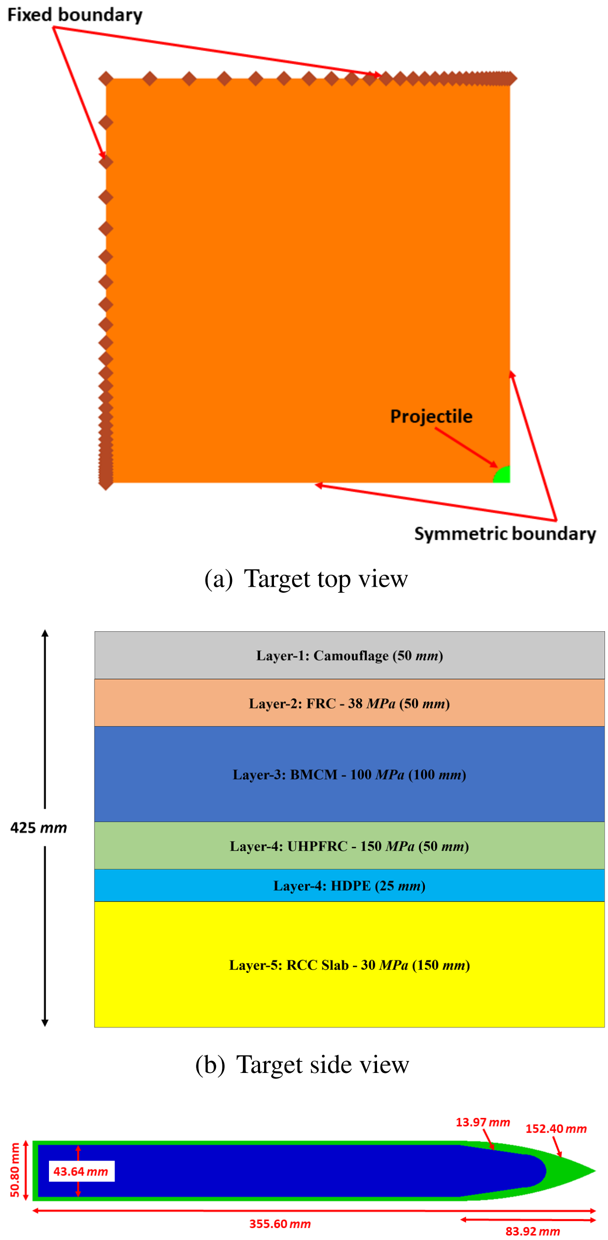

(a) Target top view

(b) Target side view

(c) Projectile geometry

Figure 1: Geometry details

The first target consisted of a reinforced concrete monolayer of equivalent thickness with dimensions of 1200 mm × 1200 mm × 340 mm. The second target was a multilayer composite with dimensions of 1200 mm × 1200 mm × 425 mm. The layered composite target was composed of distinct layers with varying thicknesses. The configuration started with a 50 mm thick camouflage (soil) layer, followed by a 50 mm thick layer of fiber-reinforced concrete (FRC). Next, a 100 mm thick layer of boulder-mixed cement mortar (BMCM) with a boulder strength of 100 MPa was added. This was followed by a 50 mm thick layer of ultra-high-performance fiber reinforced concrete (UHPFRC) and a 25 mm thick layer of high-density polyethylene (HDPE).

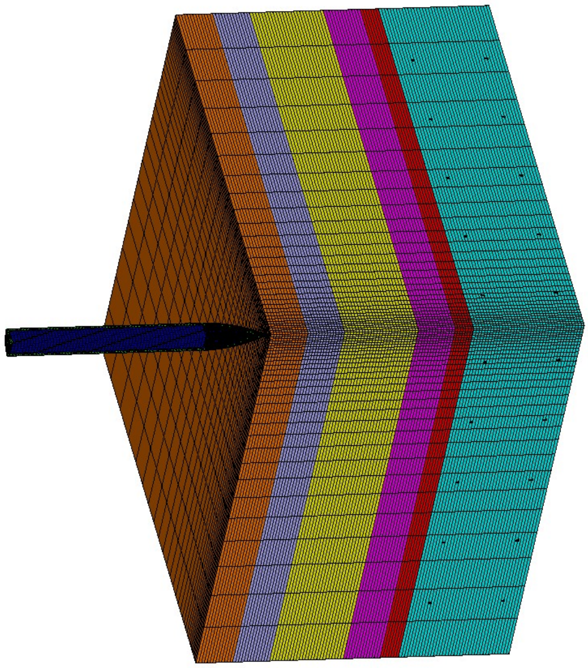

Figure 2: Mesh zoning of layered composite target.

Finally, a 150 mm thick slab of reinforced concrete with a strength of 30 MPa (RCC) was included as shown in Fig.1(b). The camouflage layer was incorporated to provide visual integration of the target with the surrounding environment, reducing its visibility [12]. The BMCM layer served as an anti-penetration layer, aiming to hinder complete penetration of the projectile into the target [6]. The HDPE layer acted as a shockwave absorber, dissipating the impact energy generated during the event [1]. Both the monolayer and layered composite targets contained reinforcement within the concrete layers. The layered composite target had two layers of reinforcement, comprising 8 mm diameter bars spaced at 110 mm center-to-center. On the other hand, the monolayer target included four layers of reinforcement with the same specifications.

The geometric modelling and meshing of the projectile was performed using Ansys Workbench, while the modeling and meshing of the reinforced concrete monolayer target, layered composite target, and reinforcement was conducted using Ansys Autodyn [13]. To optimize computational efficiency, a quarter model with two axes of symmetry was employed instead of the full model. The complete model of the projectile was initially developed, followed by the application of symmetry operations to generate the quarter model. Fixed boundary conditions were applied at the outer two faces of the target, while symmetry boundary conditions were imposed at the inner two faces as shown in Fig.1(a). Mesh zoning techniques were employed to achieve a refined mesh in the inner core region, where the projectile interacts with the target, and a coarser mesh in the outer core region as shown in Fig.2.

The reinforcement elements were modeled using beam elements, while the remaining components were represented as solid bodies. To accommodate the significant deformations arising from the projectile impact loading, an Arbitrary Lagrangian Eulerian (ALE) processor was employed. The interaction between surfaces was simulated using the gap interaction method, where each surface segment was associated with a contact detection zone that determined the initial separation between parts. Nodes entering the contact detection zone experienced repulsive forces proportional to their penetration depth into the zone and normal to the surface segment, ensuring conservation of linear and angular momentum. Gauge points were strategically assigned along the z-direction to both the monolayer reinforced concrete target and the layered composite target, allowing the extraction of desired outputs. The material model adopted in this study is as shown in the Table 1.

Table 1: Material model summary.

S.No.	Material	Equation of State	Strength Model	Failure Model
1.	Camouflage (soil) [13]	Compaction	MO Granular	Hydro (Pmin)
2.	MS Plate [14]	Shock	Johnson Cook	Johnson Cook
3.	FRC / BMCM UHPRFC/Concrete [15]	P alpha	RHT Concrete	RHT Concrete
4.	HDPE [16]	Shock	Bi-linear hardening	Plastic strain
5.	Filler (Projectile) [11]	Linear	von Mises	-
6.	Casing (Projectile) [11]	Linear	von Mises	-
7.	Reinforcement [17]	Linear	Johnson Cook	-

3 NUMERICAL VALIDATION

3.1 Single layer target

To validate the monolayer numerical model, the experimental results from Hanchak et al. [10] were utilized in a preliminary analysis. Hanchak et al. conducted a study where an ogival-nose steel projectile with a 30 mm caliber and an ogive radius of 76.2 mm as shown in Fig.3(c) impacted targets at velocities ranging from 330 m/s to 1100 m/s.

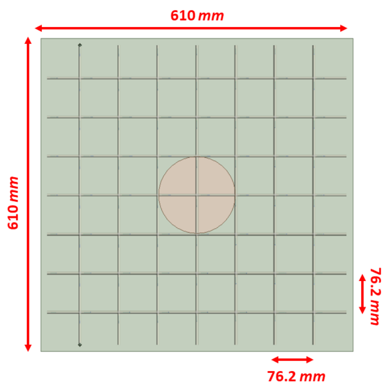

(a) In plane reinforcement

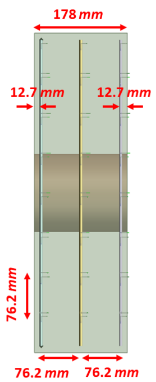

(b) Out of plane reinforcement

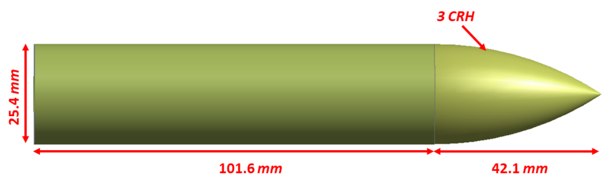

(c) Projectile geometry

Figure 3: Geometry and reinforcement details

The projectile had a total mass of 0.50 kg. The targets consisted of reinforced concrete with strengths of 48 MPa and 140 MPa. The dimensions of the reinforced concrete target were 610 mm × 610 mm × 178 mm. Steel bars with a diameter of 5.69 mm were used for reinforcement, with in-plane and out-of-plane spacing of 76.2 mm as shown in Fig.3(a) and Fig.3(b).

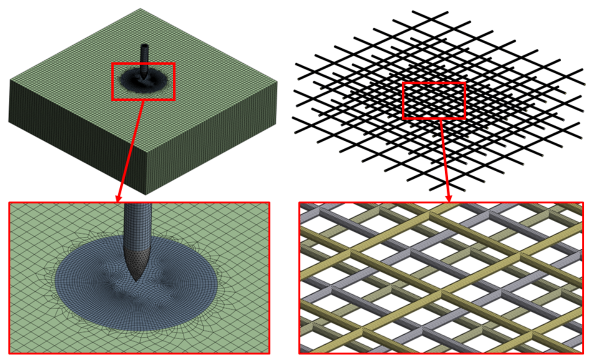

Figure 4: Meshing details

The meshing of the projectile was divided into two parts for improved accuracy. The front portion of the projectile was meshed using tetrahedral elements, while the rear body was meshed using the automatic meshing technique, employing a sweep type method. The sweep type method involved initially meshing the surface with quad/tri elements, which were then swept through the volume.

Similarly, the reinforced concrete was meshed using the sweep type method. The central region, where the projectile impacted the target, was assigned a finer element size to ensure precise capturing of results, as this area was of particular interest. The reinforcement was meshed using the automatic method, utilizing circular meshing on the surface, which was

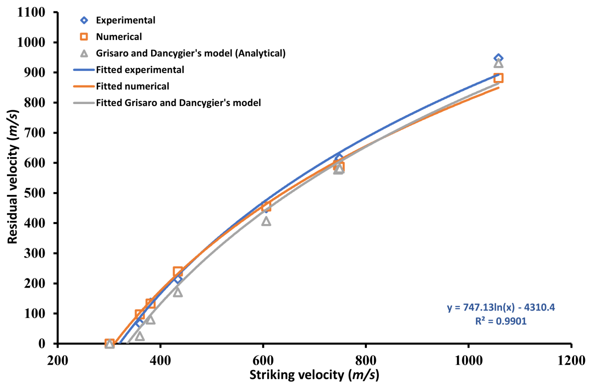

(a) 48 MPa concrete strength

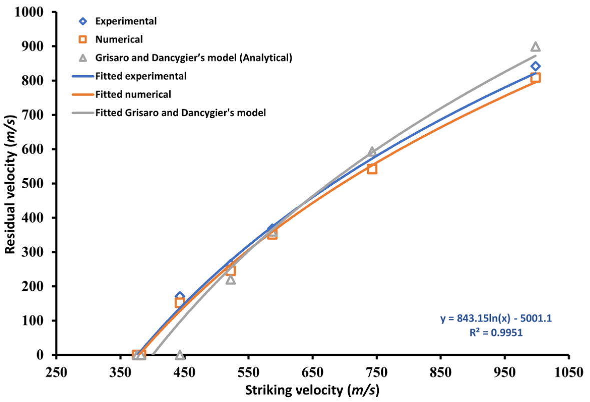

(b) 140 MPa concrete strength

Figure 5: Ballistic curve

subsequently swept through the body as shown in Fig.4. The validation has been presented here in the form of ballistic curve as shown in Fig.5.

3.2 Layered target

To validate the numerical model for the layered composite target, the experimental findings of Kamal et al. [18] were employed. Kamal et al. conducted a study in which a steel blunt nose projectile with a caliber of 23 mm impacted concrete blocks reinforced with varying numbers of layers of woven wire steel mesh (Ferrocement), as depicted in Fig.6.

The projectile had a total mass of 175 g, and it struck the concrete blocks at a velocity of 980 m/s. The dimensions of the concrete target were 550 mm × 550 mm × 400 mm.

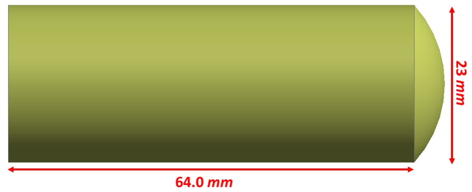

(a) Projectile geometry

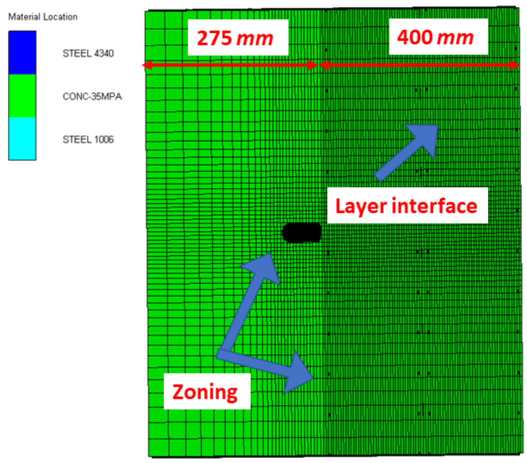

(b) Target geometry and meshing

Figure 6: Projectile and target geometry.

The reinforcement consisted of layers of steel mesh measuring 500 mm × 500 mm, with a wire diameter of 2 mm and a square opening size of 50 mm. The experiment utilized two concrete blocks positioned back-to-back, with configurations comprising zero, four, eight, and twelve layers of woven steel mesh.

The experimental tests were conducted on four different configurations of concrete blocks, with and without steel mesh reinforcement, as described earlier. Measurements of depth of penetration, residual velocity, and crater diameter were obtained for each configuration at the specified impact velocity, as presented in Table 2. In the numerical simulations, a half model was utilized instead of a quarter model for improved accuracy. The results obtained from the numerical simulations were in good agreement with the experimental results. It was observed that an increase in the number of layers of steel

Table 2: Experimental and numerical depth of penetration (DOP) and crater diameter of samples.

S No.	Sample	Depth of penetration (mm)		Percentage variation (%)	Crater diameter (mm)	
		Experimental	Numerical		Experimental	Numerical
1.	SW2-3	280	274.7	-1.89	290/fine crack	324/fine crack
2.	SW1-2	287	285.14	-0.65	325/fine crack	327/fine crack
3.	SW1-1	290	288.64	-0.47	355/fine crack	330/fine crack
4.	SC-2	400	400	0.0	550/550	333/226

mesh resulted in a decrease in both the depth of penetration and crater diameter. This indicates an improvement in the penetration resistance of the concrete block when reinforced with steel mesh.

4 RESULTS AND DISCUSSION

4.1 Mesh convergence study

The next crucial step is to conduct a mesh convergence study, which is essential for accurate and reliable numerical simulations in projectile impact loading [19].

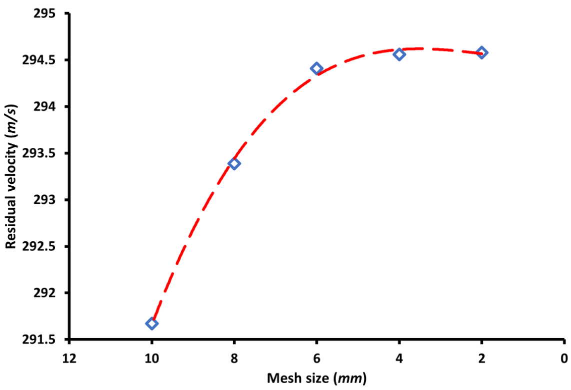

Figure 7: Mesh convergence plot of single layer target against projectile impact.

In this study, the FRC layer of the layered configuration, as illustrated in Fig.1(b), was modeled using varying mesh sizes of 10 mm, 8 mm, 6 mm, 4 mm, and 2 mm. Specifically, these mesh sizes were applied to the inner portion of the target, which is the area of interest where the projectile impacts, as mentioned in the validation section of the paper. The mesh size of the outer portion of the target was fixed at 20 mm. All other input parameters remained constant while varying the mesh size of the inner portion of the target. Numerical simulations were performed, and the resulting residual velocity, which served as the output, was recorded for each mesh size and plotted as shown in Fig.7. The analysis revealed that the output converged at a mesh size of 4 mm.

4.2 Ballistic performance

In this subsection, the ballistic limit was determined first for which impact velocity must be greater than the ballistic velocity [20]. The ballistic limit, defined as the minimum impact velocity required to perforate the target, was determined through the numerical simulation of projectile impact on the layered composite target. The residual velocity at various impact velocities was obtained from the simulation [21] and plotted as shown in Fig.8(a). A logarithmic trendline was fitted to the data points of residual velocity and impact velocity. By setting the residual velocity to zero in the logarithmic equation, the impact velocity corresponding to zero residual velocity was identified as the ballistic limit of the layered target which came out to be 1230 m/s.

Furthermore, the ballistic performance of the layered composite was determined in terms of penetration depth (DOP), end slab deflection (ESD) and deformed projectile length (DPL) for impact velocity less than the ballistic velocity as shown in Fig.8(b), Fig.8(c), and Fig.8(d). Increasing impact velocity correlates with higher depth of penetration and greater deflection of the end slab, while simultaneously leading to a decrease in the length of the deformed projectile.

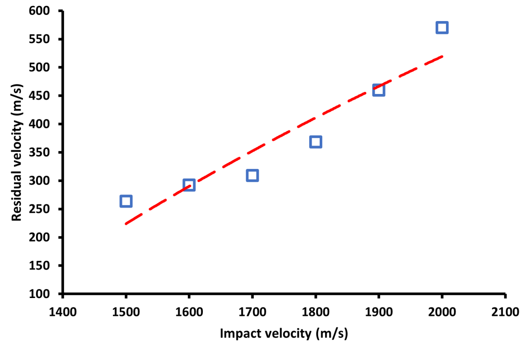

(a) Ballistic limit velocity.

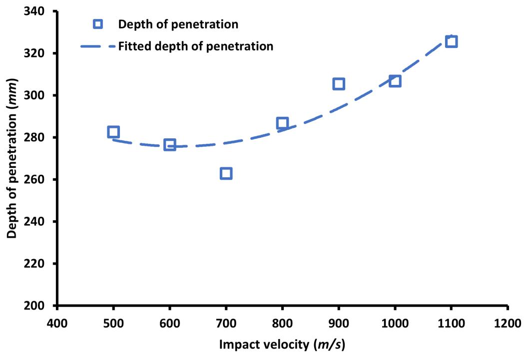

(b) Penetration depth.

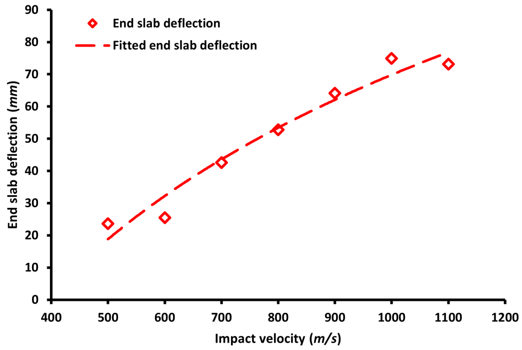

(c) End slab deflection.

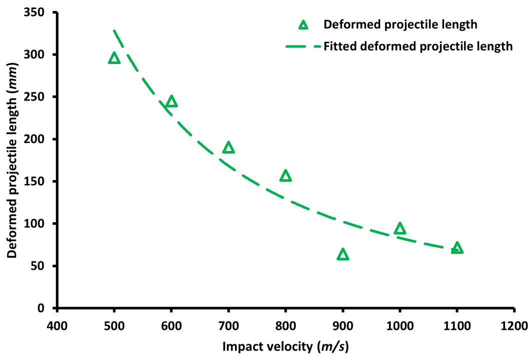

(d) Deformed projectile length.

Figure 8: Ballistic performance of the layered composite target at varying strain-rate.

4.3 Dynamic fracture behavior

The dynamic fracture behavior of the individual layers in a layered composite target under projectile impact loading plays a crucial role in determining the overall performance and protective capabilities of the structure. Each layer within the composite target exhibits unique fracture characteristics and contributes to the overall resistance against projectile penetration.

The investigation of fragment velocities under different impact velocities reveals interesting findings. Fig.9(b) illustrates that the average velocity of fragments exhibits a linear increase as the initial impact velocity rises. Remarkably, the slope of the fitted line is notably lower than 1, suggesting that the initial impact velocity is significantly higher than the average velocity of the fragments. Similarly, the maximum velocity of the fragments also shows a linear relationship with the initial impact velocity as shown in Fig.9(c) and Fig.9(a). These findings provide valuable insights into the dynamic behavior of fragments and their velocities in response to varying impact velocities and Fig.9(d) presents the investigation of fragment distribution under different impact velocities reveals noteworthy trends. As shown in Fig.9(d), the number of large fragments exhibits a linear increase. However, a slight decrease and increase in the number of small fragments is observed within the impact velocity range of 500 m/s to 2000 m/s. This decrease and increase coincides with the change in the number of large fragments.As the impact velocity increases, the number of large fragments gradually rises. Subsequently, when the impact velocity surpasses 700 m/s, the number of large fragments reaches its peak value, approximately 200, after which it experiences a continuous decrease. It is essential to note that large fragments pose a higher danger coefficient due to their potential for greater destructive power and impact force, thereby posing significant threats to the military personnel. These observed trends in fragment distribution under varying impact velocities provide valuable insights into the dynamics of the fragmentation

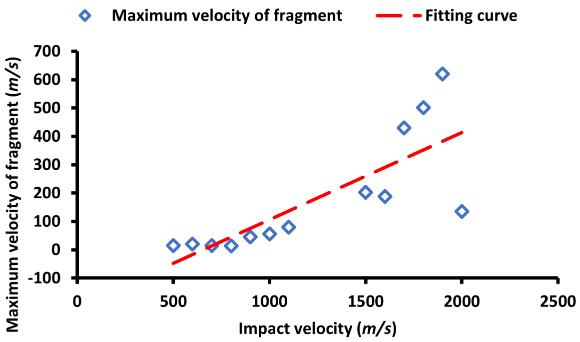

(a) Maximum velocity of fragment

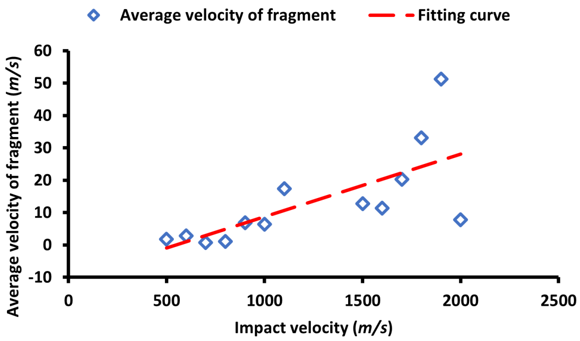

(b) Average velocity of fragment

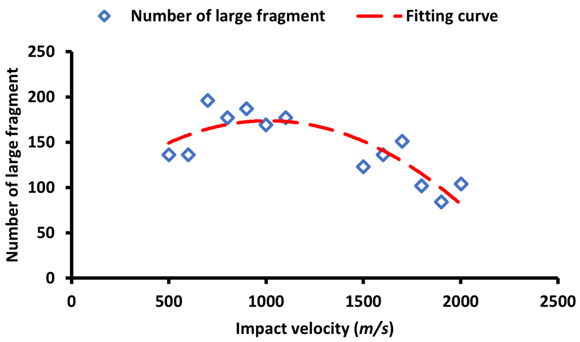

(c) Number of large fragment

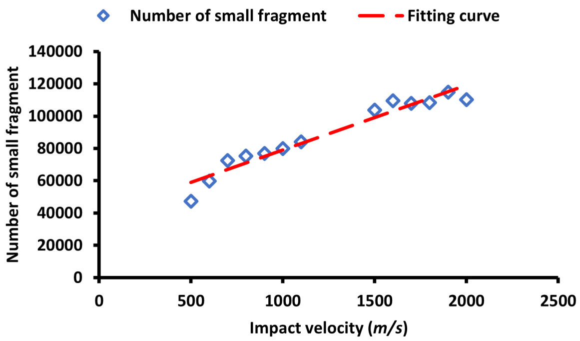

(d) Number of small fragment

Figure 9: Dynamic fracture at varying strain-rate.

process, which is crucial for understanding the potential hazards associated with impact events in different scenarios [22].

4.4 Performance in terms of target penetration

In this section, the results of the numerical simulations investigating the impact of a projectile on both the reinforced concrete monolayer target and the layered composite target were presented. The analysis focused on determining the equivalent diameter of the damage area on the front and rear surfaces of the targets, as well as the depth of penetration. These values were summarized in Table 3. The equivalent damage area diameter was calculated using the formula:

$$D_{eq} = 2 \times \frac{R_1 + R_2}{2} \qquad (1)$$

Here, R_1 represents the damage area radius along the y-axis, R_2 represents the damage area radius along the x-axis, and D_{eq} corresponds to the equivalent damage diameter.

The comparison between the monolayer target and the layered composite target revealed differences in the equivalent damage diameter on the front face and the rear face. The fully damaged area was represented by the red portion, while the undamaged area was depicted in blue in Fig.10. The damage at the end slab of the layered target was due to the bending of the slab while the damage in the monolayer target was due to the energy absorbed by the target.

In the layered target, most of the energy was being absorbed by the BMCM layer thus the damage on the rear face was developed due to bending tension as shown in Fig.10(c). Additionally, The results indicate that the projectile experienced an earlier cessation of motion when impacting the multilayer target compared to the monolayer target. This observation suggests that the rate of deceleration of the

Table 3: Equivalent diameter of damage area of monolayer target and layered composite target post impact.

Target type	Target thickness (mm)	Front face			Rear face			Depth of penetration (mm) with % penetration
		R_1 (mm)	R_2 (mm)	Equivalent damage diameter (mm)	R_1 (mm)	R_2 (mm)	Equivalent damage diameter (mm)	
Monolayer target (30 MPa)	340	170	150	320	150	190	340 (spalling)	210.90 (62.03%)
Layered composite target (end slab)	425	Nil	Nil	Nil	330	330	660 (cracks)	193.71 (45.58 %)

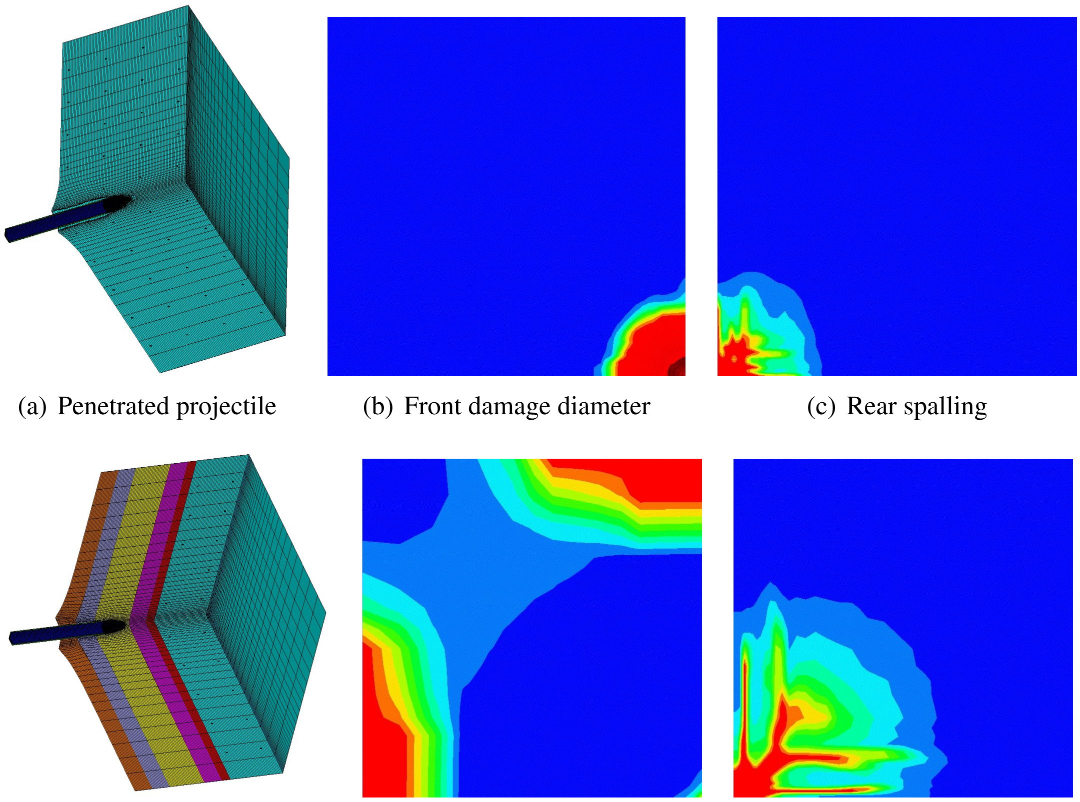

(a) Penetrated projectile (b) Front damage diameter (c) Rear spalling

(d) Penetrated projectile (e) RCC slab front damage (f) RCC slab rear spalling & crack

Figure 10: Penetration depth and damage diameter of monolayer and layered composite target.

projectile was significantly higher in the case of the multilayer target. The deceleration can be quantified as the slope of the velocity profile, demonstrating the rapid reduction in projectile velocity upon impact with the multilayer target. Such findings highlight the effectiveness of the multilayer configuration in absorbing and dissipating the projectile's kinetic energy, leading to a more abrupt decrease in its velocity compared to the monolayer target as shown in Fig.11(a). Scabbing was observed on the rear face of the monolayer target, whereas tensile cracks occurred in the layered target. The penetration depth of the layered composite target was determined to be 193.71 mm (45.58%), while the monolayer composite target exhibited a penetration depth of 210.90 mm (62.03%).

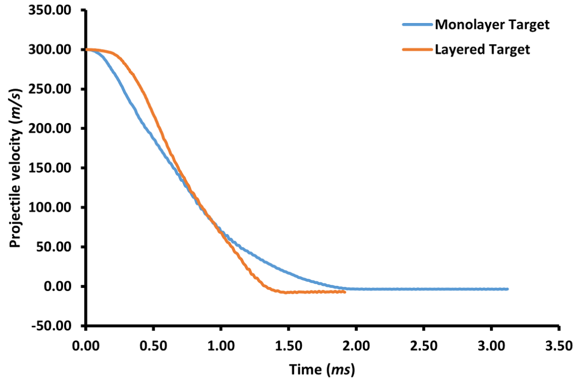

(a) Velocity profile of monolayer and layered target.

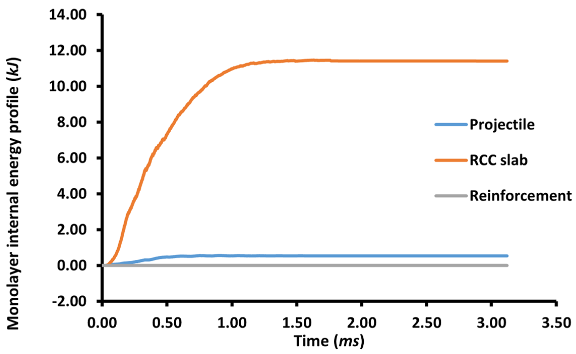

(b) Monolayer target internal energy profile.

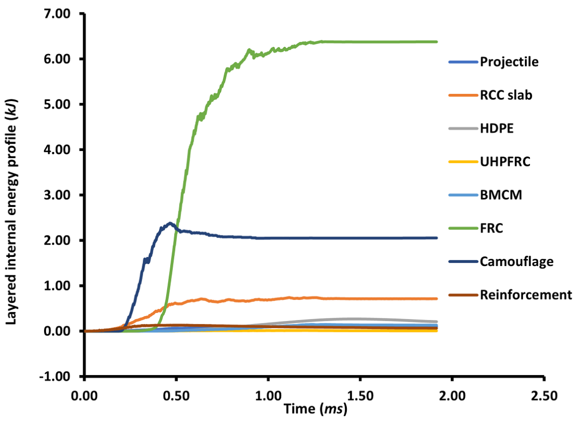

(c) layered target internal energy profile.

Figure 11: Monolayer and layered target comparison in velocity profile and internal energy profile.

5 CONCLUSION

In this research, numerical study was carried out to model the dynamic impact-induced fragmentation phenomenon in layered composite target. The study extensively explored the ballistic performance, fragment behavior under varying strain-rate, and performance in terms of target penetration. The key findings can be summarized as follows:

1. Layered composite target possess good ballistic performance under varying strain-rate condition. The ballistic limit velocity of the proposed layered target configuration came out to be 1230 m/s.

2. Important parameters such as depth of penetration (DOP), end slab deflection (ESD), and the deformed projectile length (DPL) were predicted with varying impact velocities lower than the ballistic limit velocity of the layered target.

3. The study comprehensively analyzed the characteristics of the generated fragments and their behavior during flight at varying strain-rate.

4. The layered composite targets exhibited superior performance when subjected to projectile impact loading. These targets demonstrated enhanced penetration resistance and minimal damage area diameter compared to the reinforced concrete monolayer target. Therefore, it is recommended to replace the monolayer reinforced concrete targets with layered composite targets in bunker construction to achieve improved penetration resistance against projectile impacts with reduction in overall construction costs.

REFERENCES

[1] Anand Pai, Chandrakant R Kini, and Satish Shenoy. Development of materials and structures for shielding applications against blast and ballistic impact: A detailed review. *Thin-Walled Structures*, 179:109664, 2022.

[2] Mojtaba Sadighi and René Alderliesten. Impact fatigue, multiple and repeated low-

velocity impacts on frp composites: A review. *Composite Structures*, 297:115962, 2022.

[3] Eduardo Almansa and Manuel Cánovas. Behaviour of normal and steel fiber-reinforced concrete under impact of small projectiles. *Cement and Concrete Research*, 29(11):1807–1814, 11 1999.

[4] Jeong-Ii Choi, Se-Eon Park, Huy Nguyen, Do Yun Lee, and Gyu-Yong Kim. Resistance of hybrid layered composite panels composed of fiber-reinforced cementitious composites against high-velocity projectile impact. *Composite Structures*, 281:114993, 2 2022.

[5] Ali Kheyroddin, Hamid Arshadi, M R Ahadi, G. Taban, and Max A.N. Hendriks. The impact resistance of Fiber-Reinforced concrete with polypropylene fibers and GFRP wrapping. *Materials Today: Proceedings*, 45:5433–5438, 1 2021.

[6] Jianzhong Lai, Yang Haoruo, Huifang Wang, Yuanchao Wang, and Qiang Wang. Penetration experiments and simulation of three-layer functionally graded cementitious composite subjected to multiple projectile impacts. *Construction and Building Materials*, 196:499–511, 1 2019.

[7] Ulrika Nyström and Kent Gylltoft. Comparative numerical studies of projectile impacts on plain and steel-fibre reinforced concrete. *International Journal of Impact Engineering*, 38(2-3):95–105, 2 2011.

[8] Hideki Ueno, Minako Beppu, and A. Ogawa. A method for evaluating the local failure of short polypropylene fiber-reinforced concrete plates subjected to high-velocity impact with a steel projectile. *International Journal of Impact Engineering*, 105:68–79, 7 2017.

[9] Fei Zhou, Hao Wu, and Yuehua Cheng. Perforation studies of concrete panel under high velocity projectile impact based on an improved dynamic constitutive model. *Defence Technology*, 2022.

[10] Stephen.John. Hanchak, Michael. James. Forrestal, E.R. Young, and John.Qua. Ehrgott. Perforation of concrete slabs with 48 MPa (7 ksi) and 140 MPa (20 ksi) unconfined compressive strengths. *International Journal of Impact Engineering*, 12(1):1–7, 1 1992.

[11] Choy Yoong Tham. Numerical and empirical approach in predicting the penetration of a concrete target by an ogive-nosed projectile. *Finite Elements in Analysis and Design*, 42(14-15):1258–1268, 10 2006.

[12] George T Williams, Ben M Kennedy, David Lallemant, Thomas M Wilson, Nicole Allen, Allan Scott, and Susanna F Jenkins. Tephra cushioning of ballistic impacts: Quantifying building vulnerability through pneumatic cannon experiments and multiple fragility curve fitting approaches. *Journal of Volcanology and Geothermal Research*, 388:106711, 2019.

[13] ANSYS Inc. *ANSYS Autodyn User Manual 2022 R2*. ANSYS Inc., Canonsburg, PA, USA, 2022.

[14] Imran Yusuf. Explicit finite element analysis of high speed piston impacts, October 2016. Course Code: MECH4500.

[15] Radoslav Sovjak, Tomáš Vavřiník, Jan Zatloukal, Petr Maca, Tomáš Mičunek, and Michal Frydrỳn. Resistance of slim uhpfrc targets to projectile impact using in-service bullets. *International Journal of Impact Engineering*, 76:166–177, 2015.

[16] Huon Bornstein, Shannon Ryan, and Adrian Mouritz. Physical mechanisms for near-field blast mitigation with fluid containers: Effect of container geometry. *International journal of impact engineering*, 96:61–77, 2016.

[17] Abhishek Rajput, Mohammad Ashraf Iqbal, and NK Gupta. Ballistic performances of concrete targets subjected to long projectile impact. *Thin-Walled Structures*, 126:171–181, 2018.

[18] Ibtisam Kamal and E.M. Eltehewy. Projectile penetration of reinforced concrete blocks: Test and analysis. *Theoretical and Applied Fracture Mechanics*, 60(1):31–37, 8 2012.

[19] Fei Zhou, Yuehua Cheng, Qi Peng, and Hao Wu. Influence of steel reinforcement on the performance of an rc structure subjected to a high-velocity large-caliber projectile. In *Structures*, volume 54, pages 716–731. Elsevier, 2023.

[20] Gabi Ben-Dor, Anatoly Dubinsky, and Tov Elperin. On the Lambert–Jonas approximation for ballistic impact. *Mechanics Research Communications*, 29(2-3):137–139, 3 2002.

[21] Abhishek Rajput and Mohammad Ashraf Iqbal. Ballistic performance of plain, reinforced and pre-stressed concrete slabs under normal impact by an ogival-nosed projectile. *International journal of impact engineering*, 110:57–71, 2017.

[22] Tao Yang, Hui Ma, Lei Weng, Yang Liu, Zhaofei Chu, Penglin Zhang, Gang Jin, and Weixue Chang. Fragmentation analyses of rocks under high-velocity impacts using the combined finite-discrete element simulation. *Frontiers in Earth Science*, 10:998521, 2022.